Spectromicroscopy of boron for the optimization of boron neutron capture therapy (BNCT) for cancer

1998 J. Phys. D: Appl. Phys. 31 2642

(http://iopscience.iop.org/0022-3727/31/19/038)

J. Phys. D: Appl. Phys. **31** (1998) 2642–2647. Printed in the UK PII: S0022-3727(98)92614-6

Spectromicroscopy of boron for the optimization of boron neutron capture therapy (BNCT) for cancer

B Gilbert[a], J Redondo[a], P-A Baudat[a], G F Lorusso[b], R Andres[c], E G Van Meir[d], J-F Brunet[e], M-F Hamou[e], T Suda[c], Delio Mercanti[f], M Teresa Ciotti[f], T C Droubay[g], B P Tonner[g], P Perfetti[h], M Margaritondo[a,i] and Gelsomina De Stasio[a,h]

[a] Institut de Physique Appliquée, Ecole Polytechnique Fédérale, PH-Ecublens, CH-1015 Lausanne, Switzerland
[b] University of Wisconsin Center for X-ray Lithography, Stoughton, Wisconsin
[c] Paul Scherrer Institut, CH 5232 Villigen PSI, Switzerland
[d] Laboratory of Molecular Genetics, Winship Cancer Center, Emory University, Atlanta, GA 30322, USA
[e] Laboratory of Tumor Biology and Genetics, Neurosurgery Service, University Hospital (CHUV), CH-1011 Lausanne, Switzerland
[f] Instituto de Neurobiologia del Consiglio Nazionale delle Ricerche, Viale Marx 15, 00137 Roma, Italy
[g] Department of Physics, University of Wisconsin-Milwaukee, Milwaukee, WI 53211, USA
[h] Istituto di Struttua della Materia del CNR, Via Fosso del Cavaliere, I-00133 Roma, Italy
[i] Sincrotrone Trieste SCpA, Trieste, Italy

Received 20 March 1998, in final form 22 June 1998

Abstract. We used synchrotron spectromicroscopy to study the microscopic distribution of boron in rat brain tumour and healthy tissue in the field of boron neutron capture therapy (BNCT). The success of this experimental cancer therapy depends on the preferential uptake of ^{10}B in tumour cells after injection of a boron compound (in our case $B_{12}H_{11}SH$, or BSH). With the Mephisto (microscope à emission de photoélectrons par illumination synchrotronique de type onduleur) spectromicroscope, high-magnification imaging and chemical analysis was performed on brain tissue sections from a rat carrying an implanted brain tumour and the results were compared with inductively coupled plasma-atomic emission spectroscopy (ICP-AES) detection of boron in bulk tissue. Boron was found to have been taken up more favourably by regions of tumour rather than healthy tissue, but the resulting boron distribution in the tumour was inhomogeneous. The results demonstrate that Mephisto can perform microchemical analysis of tissue sections, detect and localize the presence of boron with submicron spatial resolution. The application of this technique to boron in brain tissue can therefore be used to evaluate the current efforts to optimize BNC therapy.

1. Introduction

Boron neutron capture therapy (BNCT) is a binary treatment for cancer based on (i) selective delivery to tumour cells of a ^{10}B enriched compound and (ii) bombardment with thermal or epithermal neutrons to induce the nuclear reaction $^{10}B + n_{thermal} \rightarrow {}^4He + {}^7Li + 2.31$ MeV. In this reaction the high-energy alpha particle and lithium ion destroy the tissue within a radius of 10 μm around each boron atom. Therefore, if boron accumulation occurs only in cancer tissue, BNCT will destroy it, sparing healthy tissue [1].

The boron compound $B_{12}H_{11}SH$ (BSH) has been selected in Europe for preliminary trials of this therapy [2]. Favourable tumour versus healthy tissue BSH ratios have been reported, based on bulk tissue averages. The results demonstrated that the boron concentration in tumour tissue can vary widely within an apparently uniform tumour region [3]. The mechanisms which could lead to such variations in BSH accumulation are not well understood at present.

For any compound to accumulate in a brain tumour it must first pass across the blood–brain barrier (BBB) which

0022-3727/98/192642+06$19.50

isolates healthy brain from large or toxic substances in the blood stream. The BBB is often disrupted or weakened in brain tumours. However, once the BBB has been crossed, the mechanism of BSH uptake by cells is unknown. In addition, it has not been conclusively determined whether BSH can become chemically bound within the cell. If BSH is bound inside the cell, its location (in cytoplasm or nucleus) can have major effects on the efficacy of the boron neutron capture therapy [4].

Such considerations point to the need for an analysis of the distribution of BSH within tumour tissue with a resolution at the subcellular level. Several different techniques have been used to study the uptake of BSH and other BNCT compounds. Secondary-ion mass spectrometry [5] and neutron capture radiography [6] are the most common. The data presented here demonstrate an alternative approach with Mephisto (microscope à emission de photoélectrons par illumination synchrotronique de type onduleur). This technique is also known as synchrotron imaging photoelectron spectromicroscopy, hereafter referred to as spectromicroscopy [7]. The use of a synchrotron photon source allows high-magnification imaging and spectroscopic analysis, with the submicron resolution essential to tissue analysis at the subcellular level. This technique can be considered complementary to those previously mentioned. It is not quantitative because the signal from an element at the absorption edge of that element has large background contribution from all other elements with absorption edges at lower energies. The technique is able, however, to provide information about the chemical state of the analyte, through the position and lineshape of the absorption features.

An experiment rat brain tumour was chosen as a model for human brain cancer [8]. The aim of our present experiment was to investigate the distribution of boron in healthy and tumour tissues, and to access the capability of Mephisto to perform such a study. Biological samples can be studied directly, after dehydration for ultra high vacuum compatibility, but in this work tissue samples were ashed in an oxygen plasma to increase the relative concentration of boron.

2. Materials and methods

The tumour model used was an experimentally implanted glioma in a Wistar rat. Tumour cells were implanted into the rat to induce a malignant cancer. 4×10^6 C6 glioma cells (ATCC#CCL107) were stereotactically injected into the rat right-hemisphere striatum at a depth of 5.5 mm, 0.2 mm anterior and 3.2 mm lateral to the bregma. Twelve days after implantation and tumour growth, the rat was intraperitoneally injected with 150 mg of ^{10}B enriched BSH ($Cs_2B_{12}H_{11}SH$, Boron Biologicals Inc.) in 3 ml of isotonic solution. A further 2 h after injection, the rat was sacrificed and the brain dissected. Tissue samples were taken from the contralateral hemisphere and the tumour. A portion of each tissue sample was removed for ICP-AES analysis of the bulk boron content. Each sample was cryofixed by immersion in 2-methyl-butane at liquid nitrogen temperature and cut into 5–7 μm sections.

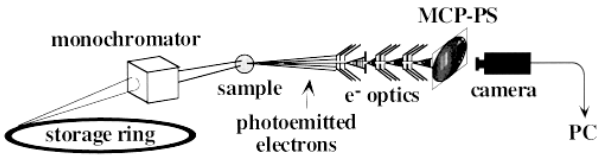

Figure 1. Schematic diagram of the Mephisto spectromicroscope.

Alternate sections were taken for histological examination or analysis with Mephisto. The specimens for histological analysis were mounted on a glass side and stained with methylene blue. The Mephisto specimens were mounted on silicon wafer substrates and ashed with a cold oxygen plasma (150 °C, Plasma-Processor 300E, Techn. Plasma GmbH, Munich) for 24 h [9].

The inductively coupled plasma-atomic emission spectroscopy (ICP-AES) analysis was performed at the ICMA, University of Lausanne, using a Perkin-Elmer Plasma 1000. Boron was detected at the emission wavelength of 249.773 mm. Weighed tissue pieces were digested in 1N nitric acid with sonication, and 9 or 13 readings were made on the resulting solution.

The Mephisto spectromicroscope (figure 1) uses an electron optics system to form a magnified image of the photoelectrons emitted by a specimen under soft x-ray illumination. The electron image intensity is amplified by a series of two microchannel plates, and is converted into a visible image by a phosphor screen. The visible image is captured by a video camera linked to a PC for display and data acquisition. The image magnification is continuously variable up to 8000× and the lateral resolution has been measured to be 40 nm [7]. Total yield spectra (primary and secondary photoelectrons are collected) as a function of photon energy can be acquired simultaneously from individual areas of a photoelectron image. Such spectra, known as x-ray absorption spectra (XAS), reflect the x-ray absorption coefficient of a layer of material at the specimen surface [10]. The probing depth, constrained by the escape depth of the secondary electrons, is of the order of 10 nm. The energy position and lineshape of XAS spectral features provide element identification and chemical state information. The absorption spectra are normalized to remove the monochromator contribution by dividing by a spectrum taken on a sputtered silicon surface.

The optical micrographs were obtained using a Zeiss Axiotech 100 HD microscope with 100× magnification. The microscope was connected to a Sony 950 DXC colour video camera whose output was captured using Avid VideoShop software for the Macintosh.

3. Results

Three tissue sections of rat brain tissue were carefully analysed with Mephisto. One section taken from tissue close to the implantation site contained both healthy and tumour tissue. A section from the contralateral hemisphere and one from the cerebellum, neither containing any tumour tissue, were also analysed. Each specimen studied was

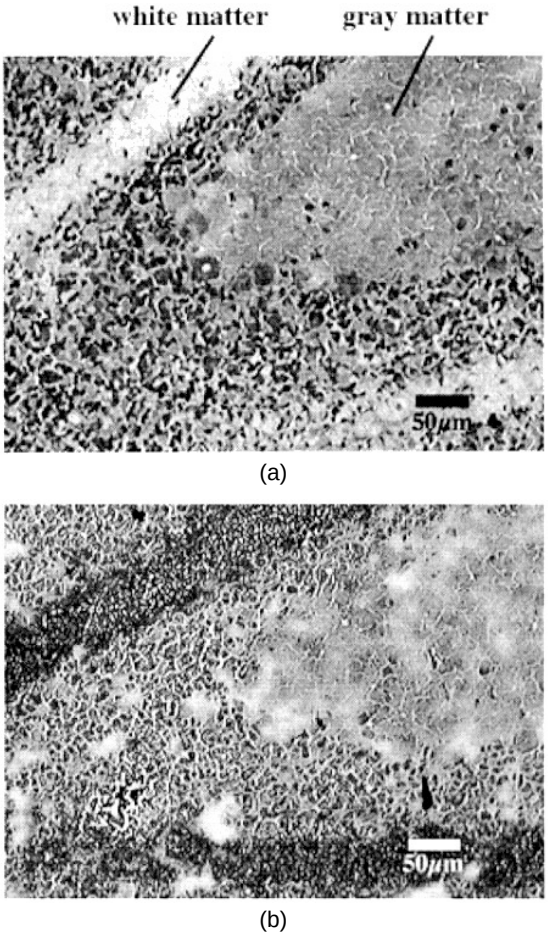

Figure 2. (a) Optical micrograph of a rat cerebelum section, stained with methylene blue. The regions of white and grey matter are clearly visible. (b) Optical micrograph of the neighbouring tissue section to (a). This tissue was ashed in an oxygen plasma for 24 h to remove organic carbon. The same regions seen in (a) remain visible, although the contrast is inverted with respect to the stained section.

chosen from a series of adjacent tissue sections which had been alternately prepared for Mephisto or histological analysis.

The optical micrographs in figures 2(a) and 2(b) were taken on two neighbouring sections from the cerebellum. The tissue in figure 2(a) was mounted on a glass slide and stained with methylene blue immediately after sectioning; that in figure 2(b) was mounted on silicon and ashed. The regions of white and grey matter emphasized by staining are also clearly visible in the ashed unstained section. The two images show excellent agreement, indicating that the ashing process does not lead to deterioration of large-scale tissue structure. The discrepancies which can be seen are likely to be due to the sectioning and mounting procedures, which may cause tissue damage to each slice before ashing.

The comparison can be extended to smaller-scale structures. The mosaic-like pattern of individual cells is also well conserved in the ashed specimen. We tentatively interpret the fine structure in figure 2(b) as intracellular gaps resulting from ashing of the aqueous intracellular compartment.

Previous data [9] demonstrated that the ashing of biological tissue removes organic carbon and enhances the spectroscopic signal from minority or trace elements and that no displacement of material occurs. The present images demonstrate that, during ashing, tissue morphology is well conserved down to the scale of individual cells, and remains comparable to unashed tissue.

Histological examination of a stained brain tissue section containing a region of tumour showed a well confined tumour which did not visibly invade the surrounding normal tissue. The results of the ICP-AES analysis of tissue boron content were 1.9 ± 0.8 ppm in tumour tissue (one sample) and 0.8 ± 0.3 ppm in the contralateral hemisphere (three samples). The higher boron concentration detected in the tumour specimen gives a tumour:healthy tissue boron concentration ratio of about 2. Other authors report tumour:healthy tissue ratios in the range 5 to 30 [11, 14] for BSH administered to rats. However, our reference histological section showed that the tissue expected to contain just tumour tissue had been cut to include only about 20–30% tumour (this is shown schematically on the adjacent tissue section of figure 5), thereby resulting in a lower measured average boron content.

Figure 3(a) is a Mephisto micrograph of a portion of tumour tissue, as identified by the histological analysis. The edge of the ashed tissue section is visible in this figure. The silicon wafer substrate appears grey and smooth, the tissue appears darker with the fine pattern we attribute to cell boundary structure. The bright border is typical of large tissue sections, which shrink on drying. Liquid that dries directly on the support leaves materials which give a high photoelectron yield, which would not be seen optically.

Figure 3(b) shows XAS spectra of the areas correspondingly labelled in figure 3(a). The areas on the image from which the spectra were taken were rectangular, with length of side 10–20 μm. For clarity, the individual spectra shown here and below have been arbitrarily displaced with respect to the ordinate axis. Curve (c), acquired from the substrate, is featureless in this energy region, indicating bare silicon. Curves (a) and (b) were both taken from tissue areas, and show spectral features at the energies corresponding to sulphur 2p, phosphorus 2s and boron 1s core levels. Sulphur and phosphorus are physiologically present, while the boron signal originates from BSH which has accumulated in the tumour tissue after injection.

The spectra in figure 3(b) can be compared with those obtained in the region of healthy tissue of the same specimen. The Mephisto micrograph of this area, figure 4(a), shows again the tissue edge and bare silicon substrate. The dark ridge of material at the edge is likely to be an artefact of the cutting or mounting processes; inside this edge in fact the healthy tissue showed less structure that the tumour tissue.

The corresponding spectra are shown in figure 4(b). Curves (a) and (b) indicate the presence of sulphur and phosphorus, but the boron absorption edge is absent. Once again the adjacent silicon surface gives a featureless spectrum in this energy range (curve (c)).

Many spectra and images were taken across this specimen. These data provide evidence of a complicated

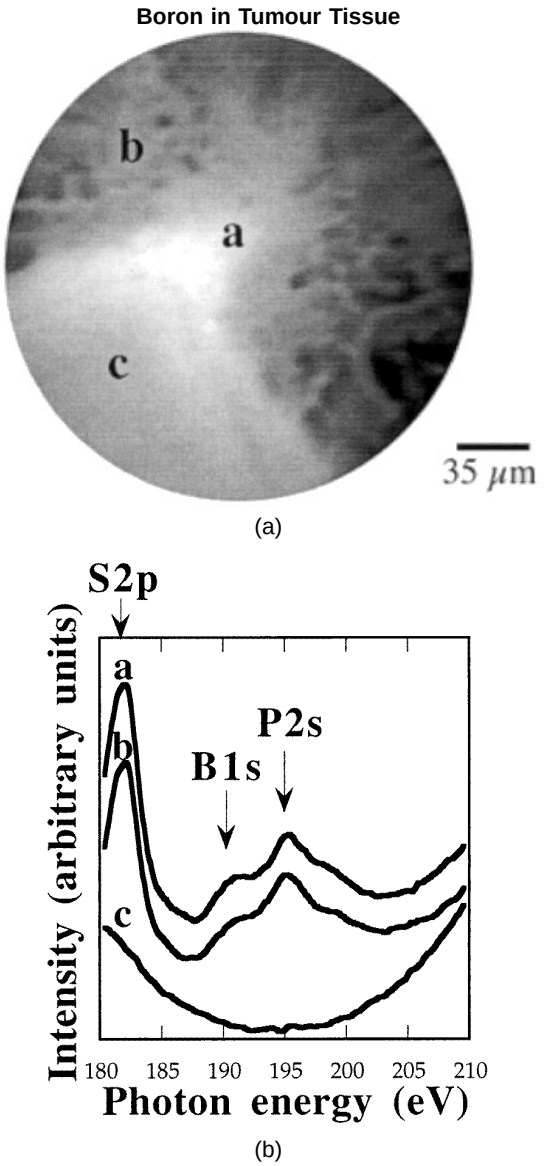

Figure 3. (a) Mephisto micrograph of the edge of tumour tissue and bare silicon support, acquired at a photon energy of 180 eV. The letters on the image indicate the areas from which total yield spectra were taken (see (b)). The contrast is topographical rather than chemical, and has been digitally enhanced. Photoelectrons from surface areas that are not perpendicular to the optical axis do not contribute to the image, and hence rough areas of cellular material appear darker than the intercellular gaps. (b) Total yield photoelectron spectra taken from the locations indicated in (a). The spectra taken from the tissue show three features, corresponding to the x-ray absorption edges of S 2p, P 2s and B 1s core electrons. The spectrum of the bare silicon wafer is featureless in this energy range, indicating that no migration of elements has occurred.

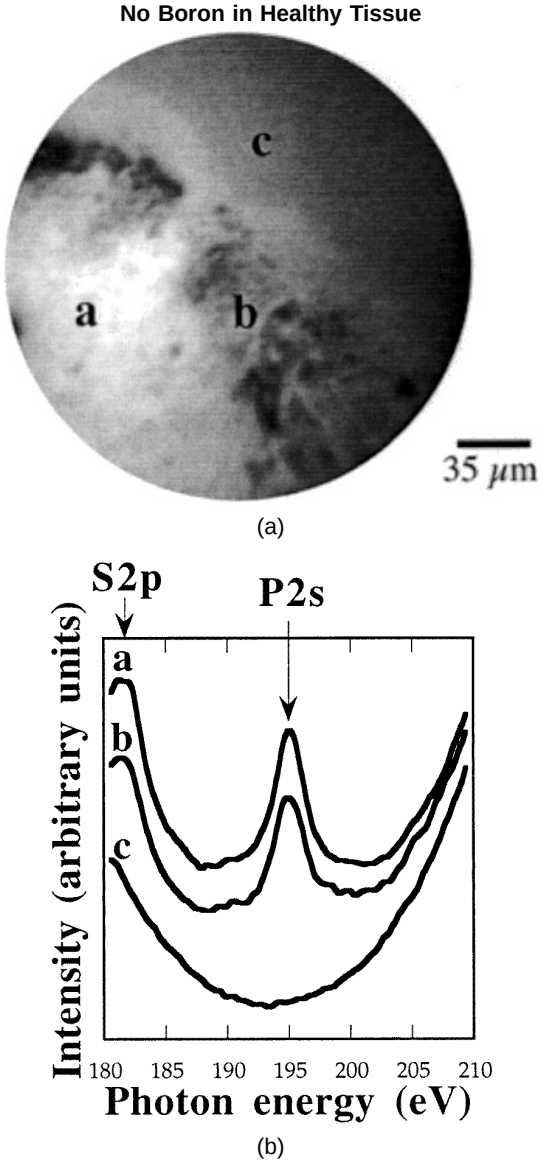

Figure 4. (a) Mephisto micrograph of the edge of healthy tissue and bare silicon support, acquired at a photon energy of 180 eV. The letters on the image indicate the areas from which total yield spectra were taken (see (b)). (b) Total yield photoelectron spectra taken from the locations indicated in (a). Features due to the absorption edges of sulphur and phosphorus are again present, but the boron signal is absent.

distribution of boron which does not simply duplicate the distribution of tumour tissue. A graphical representation of these results is given in figure 5. In this figure the outline of the specimen is shown containing the positions of the tissue areas analysed with Mephisto, and with the tumour boundary marked. Dark circles represent places in which at least one of the areas selected for spectroscopic analysis gave evidence of boron. White circles represent areas in which no boron signal was obtained. The size of the circles approximately corresponds to the Mephisto field of view that was selected for this work ($\approx$300 μm). In each of these fields we acquired one to six spectra.

Figure 5 shows fluctuation in BSH uptake on a large scale. Within individual areas of study (i.e. a single circle), additional detail was often discovered.

Figure 6(a) shows a Mephisto micrograph taken inside the region of tumour tissue, and figure 6(b) shows the corresponding XAS spectra. Spectroscopic evidence of boron can be clearly seen in the spectra obtained from two locations of this region. The bright feature (a) and a uniform area (b) both give a positive boron signal, while this signal is greatly reduced or absent from areas (c) and

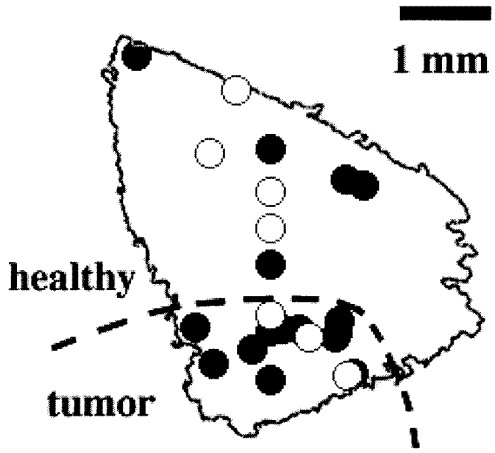

Figure 5. Graphical summary of results obtained from the tissue section containing a region of tumour. The outline of the tissue section is shown, along the approximate tumour boundary. Full circles represent regions in which at least one area analysed gave evidence of boron. Open circles represent regions which no boron was detected. When choosing the sites for analysis, care was taken to sample the tissue specimen widely to avoid selection bias.

(d). All four areas lie within a radius of no more than 50 μm. The dimensions of individual tumour cells are of the order of 20 μm.

4. Discussion

As indicated earlier, for any x-ray energy electrons with a lower binding energy will be excited and hence contribute to the total photoelectron signal. For example, the photoelectron yield from tissue at the boron K-edge contains significant contributions from both the sulphur and phosphorus L-edges. Each signal is resolved but, except for well-characterized (materials science) specimens, it is not possible to decompose the signal accurately to extract the contribution for each element. Additionally, at any location on the sample, the nature of the topography affects the efficiency with which the photoelectron yield is collected by the detector.

Nevertheless, the variation in relative signal strength between different locations on the same specimen can be interpreted as real variations in analyte concentration (the signal strength is constant over a uniform sample). Note that sulphur and phosphorus are present throughout the tissue, as can be seen in the spectra presented here. The observed variation in the ratio of boron 1s and phosphorus 2s peak heights is evidence of an inhomogeneous boron distribution.

In the analysis of other physical and biological specimens with Mephisto, it is straightforward to produce distribution maps of an element, or even an chemical species, by subtracting two photoelectron images, one acquired on an absorption edge, one at a photon energy immediately before the edge [7, 12]. During the analysis of the rat tissue sections the strength of the boron signal was insufficient, and the information about boron distribution

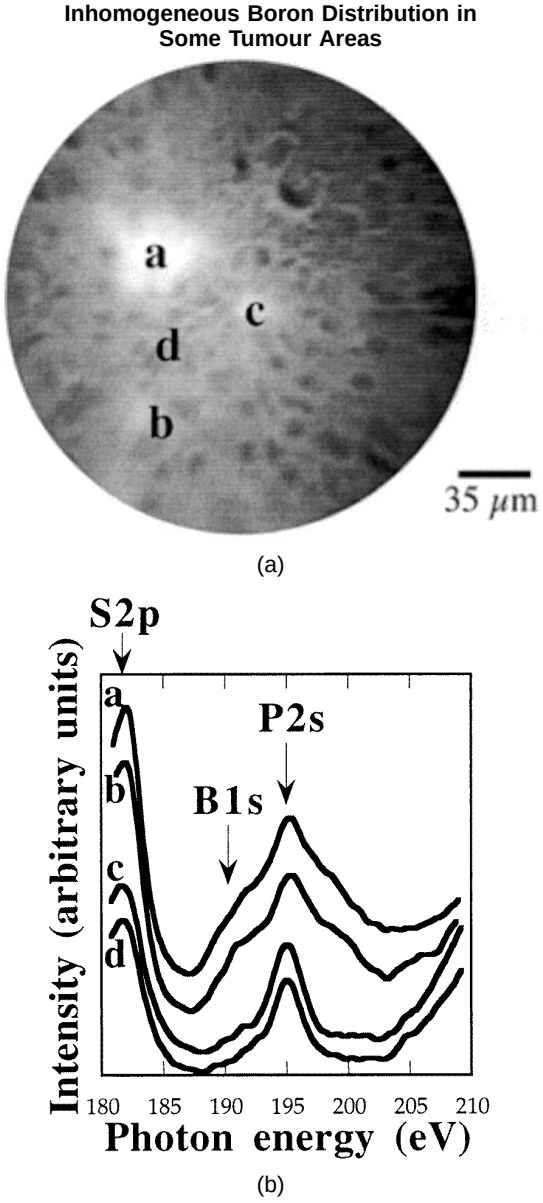

Figure 6. (a) Mephisto micrograph of an area of tumour tissue, acquired at a photon energy of 180 eV. The letters on the image indicate the areas from which total yield spectra were taken (see (b)). (b) Total yield photoelectron spectra taken from the locations indicated in (a). A strong boron signal is detected from areas a and b. By contrast, the boron signals from areas c and d are greatly lower, reflecting lower boron concentrations in these areas.

in the resulting subtraction images was obscured by noise. Extra contrast due to surface topography was also a dominant effect.

The following improvements are envisaged to allow the acquisition of boron distribution maps from tissue: the optimization of the sample preparation to produce flatter samples, the continuous upgrading of Mephisto itself, and the use of brighter synchrotron sources.

Mephisto analysis of rat brain tissue shows that BSH did not uniformly reach all tumour areas. In an apparently homogeneous tumour region, areas with no evidence of boron were found, and significant fluctuations in boron

signal were obtained from regions only tens of microns apart. Figures 5 and 6 show that, while boron was found at a higher frequency within the tumour region, spectra taken from areas inside this region did not always detect boron. In addition, boron was found in some areas of healthy tissue.

These observations are highly significant for BNCT. The biologically destructive products of the boron–neutron reaction have a range of 10 μm in tissue. To effectively kill cancer cells, alpha particles must be generated inside the cell membranes and therefore ^{10}B should accumulate inside the tumour cells [4]. Boron neutron capture reactions taking place within one cell are, however, unlikely to damage neighbouring cells. As individual surviving cancer cells could potentially produce a new tumour, a treatment must target every one.

Boron was also found in areas of healthy tissue. One possible cause for such a finding is that the rat was not perfused before sectioning, and so blood vessels lying in any tissue section could be expected to contain boron. (The initial half-life for the elimination of BSH from the blood is around 30 min [13, 14].) When an area of ashed tissue gave evidence of boron, the corresponding location on the neighbouring non-ashed stained section was studied. As no specific immunohistochemistry was employed, however, no positive identification of blood vessels could be made. Areas of boron in apparently healthy tissue could also be due to individual tumour cell infiltrations targeted by BSH [13]. The third possibility is the uptake of BSH by healthy tissue. Obviously boron in healthy cells will cause undesired cell death. Previous work with rat gliomas has detected low boron levels in bulk samples of healthy brain a few hours after injection, but the issue of the boron microdistribution was not addressed [14]. Further work is required to confidently explain the presence of boron in areas of healthy tissue. In cases of human glioma, areas of normal brain tissue have shown negligible boron content, following the administration of BSH [3, 15]. The results obtained from the rat model should therefore be applied with care to the human case.

5. Conclusions

We have demonstrated that spectromicroscopy with Mephisto can perform microchemical analysis of boron in tumour and healthy tissue specimens. With spectromicroscopy of rat glioma we observed boron in areas of tumour more frequently than in healthy tissue. This was consistent with ICP-AES analysis which detected elevated boron levels in tissue containing tumour. The BSH distribution was found to be inhomogeneous, as indicated by variations in the intensity of the boron signal from areas of tumour tissue. Areas containing boron were also discovered in apparently healthy tissue, and this was confirmed by ICP analysis of healthy tissue. The various possible causes of the presence of boron in this tissue could not be distinguished; however, such a result can still be compatible with an overall lower boron concentration in healthy tissue, as reported by other authors [13, 14].

The capability of Mephisto to provide both images and chemical information gives the technique wide application in BNCT research. Efforts are under way to investigate and optimize all aspects of the therapy. The delivery of BSH to tumour cells can vary with tumour size and type, requiring patient-specific treatment in human cases [15]. Certain compounds injected concomitantly may aid the delivery of BSH to regions of tumour [16]. Alternative boron carrying compounds are being synthesized, such as borophenylalanine (BPA) or boronated porphyrins [13, 17], potentially with a higher tumour affinity than BSH. Work in all these areas ultimately aims to achieve the highest possible concentration of boron in tumour cells only, which would allow the neutron dose to healthy tissue to be minimized. The evaluation and optimization of all these developments in BNCT is a role well suited to the flexible microanalysis technique provided by Mephisto.

Acknowledgments

Work supported by the Fonds National Suisse de la Recherche Scientifique, by the Conseglio Nazionale delle Ricerche and by the Université and Ecole Polytechnique Fédérale of Lausanne. We are indebted to Mario Capozi, Mary Severson and the entire staff of the Wisconsin Synchrotron Radiation Center (a national facility supported by the NSF under grant DMR-95-31009) for their expert professional help. We are indebted to C Jayet and B Ess for rat injections and Dr Didier Peret for assistance with the ICP-AES measurements. We thank Professor Borje Larsson for his support and advice.

References

[1] Barth R F, Soloway A H, Rairchild R G and Brugger R M 1992 *Cancer* **70** 2995–3007
[2] Gabel D 1990 *Progress in Neutron Capture Therapy for Cancer* ed B J Allen *et al* (New York: Plenum) pp 31–6
[3] Haritz D, Gabel D and Huiskamp R 1994 *Int. J. Radiat. Oncol. Biol. Phys.* **28** 1175–81
[4] Gabel D, Foster S and Fairchild R G 1987 *Radiat. Res.* **111** 14–25
[5] Smith D R, Chandra S, Coderre J A and Morrison G H 1996 *Cancer Res.* **56** 4302–6
Zha X, Ausserer W A and Morrison G H 1992 *Cancer Res.* **52** 5219–22
[6] Ceberg C P, Salford L G, Brun A, Hemler R J B and Persson B R R 1993 *Radiother. Oncol.* **26** 139–46
[7] De Stasio G, Capozi M, Lorusso G F, Baudat P-A, Droubay T C, Perfetti P, Margaritondo G and Tonner B P 1998 *Rev. Sci. Instrum.* **69** 2062–7
De Stasio G, Hardcastle S, Koranda S F, Tonner B P, Mercanti D, Ciotti M T, Perfetti P and Margaritondo G 1993 *Phys. Rev.* B **47** 2117–21
[8] San-Galli F, Vrignaud P, Robert J, Coindre J M and Cohadon F 1989 *J. Neuro-Oncol.* **7** 299–304
[9] De Stasio G *et al* 1997 *Anal. Biochem.* **252** 106–9
[10] Gudat W and Kunz C 1972 *Phys. Rev. Lett.* **29** 169–73
[11] Soloway A H, Hatanaka H and Davis M A 1967 *J. Med. Chem.* **10** 714–17
[12] De Stasio G *et al* 1993 *NeutroReport* **4** 1175–8
[13] Ceberg C P *et al* 1995 *J. Neurosurg.* **83** 86–92
[14] Clendenon N R *et al* 1990 *Neurosurgery* **26** 47–55
[15] Stragliotto G and Fankhauser H 1995 *Neurosurgery* **36** 285–93
[16] Haselberger K, Radner H and Pendl G 1996 *Neurosurgery* **39** 321–6
[17] Barth R F *et al* 1994 *Int. J. Radiat. Oncol. Biol. Phys.* **28** 1079–88